

PHYSICAL CHEMISTRY OF WATER TREATMENT PROCESSES

Photodegradation of Organophosphorus Pesticides on Magnetically Recyclable Core-Shell Nanocatalyst

Jitendra R. Satam^{a,*} and Shamrao T. Disale^b

^a Faculty of Engineering Chemistry, K.J. Somaiya College of Engineering,
Somaiya Vidyavihar University, Mumbai, 400 077 India

^b Department of Chemistry, Kankavli College, University of Mumbai,
Kankavli, Sindhudurg, 416602 (MS), India

*e-mail: jitendrasatam@somaiya.edu

Received August 24, 2023; revised February 27, 2024; accepted March 28, 2024

Abstract—Magnetically recyclable nanoparticle catalysts, in particular, Fe_3O_4 , $\text{TiO}_2@\text{Fe}_3\text{O}_4$, $\text{SiO}_2@\text{Fe}_3\text{O}_4$, $\text{TiO}_2-\text{SiO}_2@\text{Fe}_3\text{O}_4$ and silver doped $\text{TiO}_2-\text{SiO}_2@\text{Fe}_3\text{O}_4$ ($\text{Ag}-\text{TiO}_2-\text{SiO}_2@\text{Fe}_3\text{O}_4$) were synthesized by sol-gel and modified sol-gel synthesis methods. These nanoparticle catalysts were prepared from metal salts and alkoxide precursor salts. Photocatalytic activity of these catalysts was studied in the degradation of organophosphorus pesticides Glyphosate, and Malathion in water. A detailed study of photodegradation of these organic compounds under UV radiation was performed. The physicochemical characterization of the synthesized nanoparticles was performed using TEM (Transmission electron microscopy), EDX (energy dispersive X-ray), ICP-AES (inductively coupled plasma-atomic emission spectroscopy), XRD (X-ray diffraction) and BET surface area measurement techniques. The degradation reactions of organic pesticides were performed in a specially designed photo-batch reactor. The use of H_2O_2 as an oxidant in the reaction was found to enhance the catalytic performance towards degradation and subsequent mineralization of the organophosphorus pesticides. Silver-doped nanocatalyst exhibits high recycling efficiency and stability over several subsequent runs. The course of the reactions was studied using COD (chemical oxygen demand) removal and HPLC (high-performance liquid chromatography) methods of water before and after the photodegradation reactions. More than 95% reduction in the COD was observed in the treated water sample using $\text{Ag}-\text{TiO}_2-\text{SiO}_2@\text{Fe}_3\text{O}_4$.

Keywords: magnetic, core-shell, nanoparticles, photodegradation, pesticides

DOI: 10.3103/S1063455X2404009X

INTRODUCTION

Water pollution is considered to be the major cause of the degradation of the ecosystem. Industrial wastewater and agricultural runoff water contain various types of organic chemicals, in particular dyes, chlorophenols, pesticides etc. which significantly contribute to water pollution. Such chemical pollutants can cause damage to the kidney, liver and reproductive system, and also cause skin irritation and cancer in humans. Therefore removal of such harmful chemical pollutants from water is much much-needed task. These harmful chemicals could be transformed into innocuous substances by degradation and subsequent mineralization. Major types of pesticides used globally are herbicides, insecticides and fungicides which become major sources of water pollution. Appreciable amounts of these pesticides are present in groundwater and untreated potable water. Pesticides could remain in the soil or groundwater un-decomposed for several decades [1–3]. Such persistent pesticides cause detrimental effects on living organisms. We have reported some important organic transformations on surface-modified semiconducting metal oxides as catalysts [4–6]. Photocatalytic degradation by semiconducting metal oxide catalysts is found to be a useful technique for the degradation of chemical pollutants in wastewater [7–13]. In the last few decades, great efforts have been made for the treatment of pollutants using advanced oxidation processes (AOPs) using TiO_2 -mediated photocatalysis, Fenton or photo-Fenton reactions. AOPs are found to have large potential in this area [14–18]. Several reports have been published that involve heterogeneous photocatalysts using advanced oxidation techniques for the degradation of organic pollutants. The heterogeneous photocatalysis method enables the degradation of harmful organic pollutants through the photocatalytic redox reaction. Photocatalyst absorbs the photon from light having energy same as or higher than

its band gap. An electron jumped from a filled valence band to a vacant conduction band generates an electron–hole pair that further initiates redox reactions with species adsorbed on the surface of a particle. In water holes are foraged by surface hydroxyl groups (OH^-) to generate highly oxidizing species, $\cdot\text{OH}$ radicals, which results in oxidative degradation of harmful organic chemicals.

The majority of the reported methods used for the degradation of harmful organic chemicals suffer from disadvantages, being non-recyclable and presenting difficulties in separating the photocatalysts from the reaction medium during work-up. Nano iron oxide being magnetically separable has also shown great potential for the degradation of some organic chemicals, particularly chlorinated benzenes and polychlorinated biphenyls [19]. Some reports involve the use of ultrasound technique, either alone or in combination with iron-based Fenton's reagent [20]. Doping of nano iron oxide with another metal oxide was found to improve the degradation performance of pure nano iron oxide; at the same time resultant material becomes magnetically separable [21]. Various combinations of iron-based nanoparticle catalysts have been employed for the degradation of organic compounds [22]. There is a need to find an effective, convenient and practical method of degrading organophosphorus pesticides. Magnetically separable nanoparticles could be the better choice as photocatalysts for the degradation of organophosphorus pesticides if their catalytic performance is enhanced through surface modification and doping. In the current procedure, magnetically separable and recyclable silver-doped photocatalysts have been employed in the degradation of organophosphorus pesticides. This catalyst, synthesized using the sol-gel technique, was found to be an efficient one for the degradation of organophosphorus pesticides in the presence of UV (Ultraviolet) irradiation. UV irradiation upon interaction with the photocatalyst in the presence of H_2O_2 oxidant gives rise to photosensitized oxidation which further results in oxidative degradation of harmful organophosphorus pesticides in water.

EXPERIMENTAL

Reagent and Chemicals

Ethanol, ethylene glycol, citric acid, $\text{FeCl}_2 \cdot 4\text{H}_2\text{O}$, $\text{FeCl}_3 \cdot 6\text{H}_2\text{O}$, tetraethyl orthosilicate (TEOS), titanium isopropoxide (TIPO), AgNO_3 (AR Grade Chemicals were procured from SD Fine Chemicals with purity 99.9%), H_2O_2 (30% w/w, Merck), Glyphosate and Malathion pesticides were procured from local industries. All chemicals were used directly without any purification.

Preparation of Magnetically Separable Nanocatalysts

Preparation of Fe_3O_4 nanoparticles. In a typical procedure, the required amounts of $\text{FeCl}_2 \cdot 4\text{H}_2\text{O}$ and $\text{FeCl}_3 \cdot 6\text{H}_2\text{O}$ salts were dissolved in a mixture of distilled water, ethanol and ethylene glycol (10 mL each) to obtain a clear solution. This solution was aged at 60°C for about 4 h to form a gel. The gel thus obtained was diluted with 10 mL of ethanol and the mixture was transferred further into an autoclave with a capacity of 100 mL. The mixture was kept at 200°C for 8 h and slowly cooled to obtain a black precipitate, which was collected magnetically. The magnetic nanoparticles were washed first with distilled water then with ethanol and dried at 60°C for 5 h in a vacuum oven.

Preparation of $\text{SiO}_2@\text{Fe}_3\text{O}_4$ core-shell nanoparticles. As-prepared Fe_3O_4 nanoparticles (100 mg) were mixed with ethanol (20 mL) and stirred vigorously to form a homogeneous dispersion. To this, a mixture of TEOS (5 mL), aqueous HCl solution (20 mL, 1 mol L⁻¹) and ethanol (20 mL) was added at 80°C for 2 h. The obtained nanoparticles were separated magnetically and washed thoroughly with distilled water, then dried at 60°C for 5 h in a vacuum oven.

Preparation of $\text{TiO}_2@\text{Fe}_3\text{O}_4$ core-shell nanoparticles. A homogeneous dispersion of prepared Fe_3O_4 particles (100 mg) was made with 10 mL distilled water and 10 mL ethanol under vigorous stirring. A mixture of TIPO (5 mL), aqueous HCl solution (20 mL, 1 mol L⁻¹) and ethanol (20 mL) was added to the above solution at 80°C for 90 min. The particles obtained were washed first with distilled water then with ethanol and dried at 60°C for 5 h in a vacuum oven and further calcinated at 350°C for 2 h.

Preparation of $\text{TiO}_2\text{-SiO}_2@\text{Fe}_3\text{O}_4$ core-shell nanoparticles. A homogeneous dispersion of prepared $\text{SiO}_2@\text{Fe}_3\text{O}_4$ core-shell particles (100 mg) was made with 10 mL distilled water and 20 mL ethanol under vigorous stirring. A mixture of TIPO (5 mL), aqueous HCl solution (20 mL, 1 mol L⁻¹) and ethanol (20 mL) was added to the above solution at 80°C for 90 min. The particles obtained were first washed with distilled water then with ethanol and dried at 60°C for 5 h in a vacuum oven and further calcinated at 350°C for 2 h.

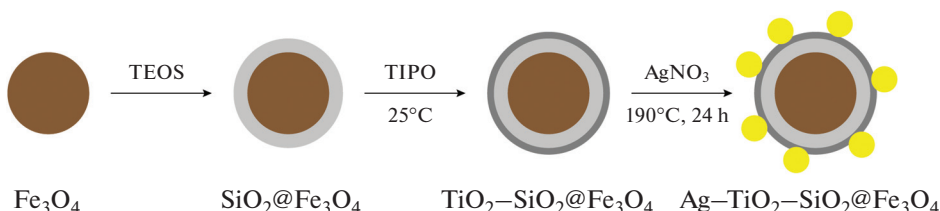


Fig. 1. Preparation of core-shell nanoparticle catalysts.

Preparation of $\text{Ag}-\text{TiO}_2-\text{SiO}_2@\text{Fe}_3\text{O}_4$ core-shell nanoparticles. Further doping with silver was achieved on the TiO_2 layer by using an aqueous AgNO_3 solution to obtain 1 wt % of Ag deposited on the surface of $\text{TiO}_2-\text{SiO}_2@\text{Fe}_3\text{O}_4$ using a hydrothermal method at 190°C in Teflon lined autoclave. The synthesized nanoparticles were separated magnetically and further calcinated at 350°C for 2 h.

The stepwise process of core-shell nanoparticle formation is shown in Fig. 1. Prepared Fe_3O_4 nanoparticles were first coated with SiO_2 nanoparticles using TEOS to obtain $\text{SiO}_2@\text{Fe}_3\text{O}_4$ which further reacted with TIPO to obtain $\text{TiO}_2-\text{SiO}_2@\text{Fe}_3\text{O}_4$. The silver deposition was achieved on $\text{TiO}_2-\text{SiO}_2@\text{Fe}_3\text{O}_4$ nanoparticles using a silver nitrate solution.

RESULTS AND DISCUSSION

Characterization of Various MNPs

These as-synthesized nanoparticle catalysts were characterized using transmission electron microscopy (TEM), EDX (energy dispersive X-ray), ICP-AES (inductively coupled plasma atomic emission spectroscopy), X-ray diffraction (XRD) and BET surface area measurement techniques. TEM and EDX images were obtained using a Philips CM-200 transmission electron microscope at a 200 kV operating voltage. ICP-AES data was obtained from SPECTRO, and XRD analysis was obtained on a conventional powder diffractometer (Philips 1050). BET surface area measurements were performed using the Micromeritics (ASAP 2010) instrument.

TEM and EDX image of $\text{Ag}-\text{TiO}_2-\text{SiO}_2@\text{Fe}_3\text{O}_4$. TEM measurement revealed that the average size of $\text{Ag}-\text{TiO}_2-\text{SiO}_2@\text{Fe}_3\text{O}_4$ core-shell nanoparticles was 120–130 nm (Fig. 2a). Silver doping on $\text{TiO}_2-\text{SiO}_2@\text{Fe}_3\text{O}_4$ is visible in the TEM image. EDX analysis of the catalyst confirms the presence of Fe, Ti, Si, Ag and O in the material (Fig. 2b). ICP-AES further confirmed that the percentage of Ag in the sample was approximately 0.97 wt %.

XRD analysis. The XRD patterns of Fe_3O_4 nanoparticles and different surface-modified Fe_3O_4 nanoparticles are represented in Fig. 3. The cubic structure of Fe_3O_4 nanoparticles was exhibited by strong diffraction peaks at $2\theta = 30.12^\circ, 35.40^\circ, 42.90^\circ, 54.10^\circ, 57.24^\circ$, and 63.24° . Silver-coated $\text{TiO}_2-\text{SiO}_2@\text{Fe}_3\text{O}_4$ particles showed several additional peaks, confirming the presence of anatase TiO_2 and silver.

BET measurements. The surface areas (m^2/g) of the catalysts are given in Table 1. It was observed that surface modification with semiconducting oxides to form a shell structure on the Fe_3O_4 core improves the surface area of the material. This could be contributed to the increase in porosity of the nanocatalysts after surface treatments. $\text{Ag}-\text{TiO}_2-\text{SiO}_2@\text{Fe}_3\text{O}_4$ was found to have a maximum surface area $56.1\text{ m}^2/\text{g}$ compared to the other catalysts used in the method.

Experimental Procedures

The degradation of Glyphosate and Malathion in water was studied using as-synthesized magnetically separable nanocatalysts in a specially designed photo batch reactor as shown in Fig. 4. For a typical reaction, 100 mg/L solution of each pesticide was used as a stock solution. The degradation study with and without catalysts was performed. $\text{Ag}-\text{TiO}_2-\text{SiO}_2@\text{Fe}_3\text{O}_4$ catalyst was found to be a superior photocatalyst compared to the other nanoparticles used in the methodology.

Not much photodegradation was observed when the reaction was performed in the absence of any catalyst. Figure 5 represents the degradation course of various as-synthesized catalysts for the photodegradation of Glyphosate and Malathion in water under UV irradiation using medium-pressure mercury lamp,

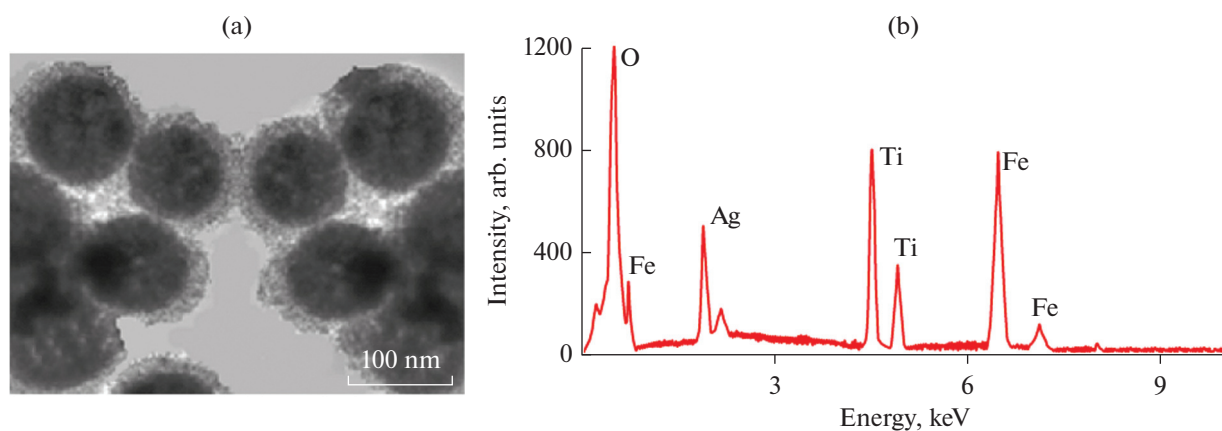


Fig. 2. (a) TEM image and (b) EDX result of $\text{Ag}-\text{TiO}_2-\text{SiO}_2@\text{Fe}_3\text{O}_4$.

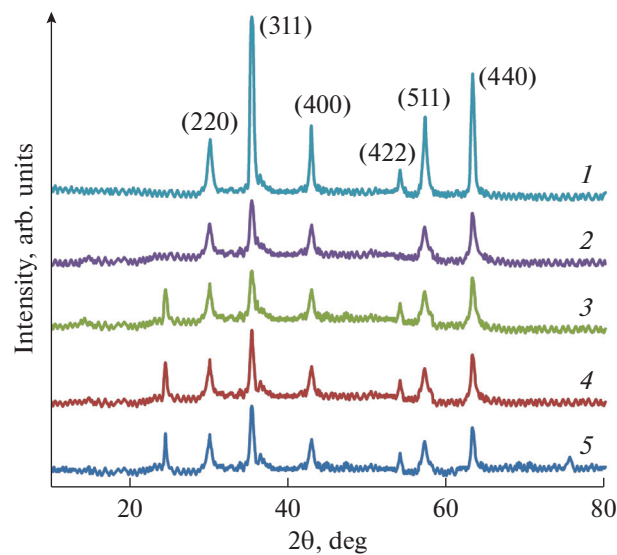


Fig. 3. XRD of (1) Fe_3O_4 , (2) $\text{SiO}_2@\text{Fe}_3\text{O}_4$, (3) $\text{TiO}_2@\text{Fe}_3\text{O}_4$, (4) $\text{TiO}_2-\text{SiO}_2@\text{Fe}_3\text{O}_4$, (5) $\text{Ag}-\text{TiO}_2-\text{SiO}_2@\text{Fe}_3\text{O}_4$.

UV light range (250–400 nm). Silver doping was found to increase the photodegradation performance of the catalysts. It was observed that in the presence of $\text{Ag}-\text{TiO}_2-\text{SiO}_2@\text{Fe}_3\text{O}_4$ catalyst, photodegradation of Glyphosate could be completed in 100 min, while photodegradation of Malathion was achieved in 6 h (Fig. 5). $\text{Ag}-\text{TiO}_2-\text{SiO}_2@\text{Fe}_3\text{O}_4$ was found to be more efficient compared to the other photocatalysts used for the degradation of pesticides. The COD removal tests of water before and after the degradation reactions were performed to test the further toxicity of treated water.

Table 1. Surface area of magnetic nanocatalysts

Catalyst	Surface Area, m^2/g
Fe_3O_4	10.4
$\text{TiO}_2@\text{Fe}_3\text{O}_4$	24.2
$\text{SiO}_2@\text{Fe}_3\text{O}_4$	16.4
$\text{TiO}_2-\text{SiO}_2@\text{Fe}_3\text{O}_4$	45.5
$\text{Ag}-\text{TiO}_2-\text{SiO}_2@\text{Fe}_3\text{O}_4$	56.1

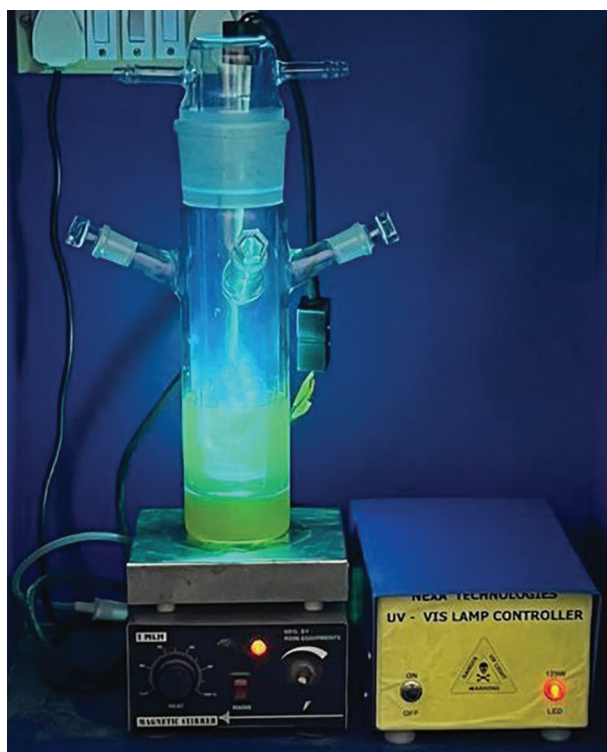


Fig. 4. Photodegradation reaction performed in the presence of catalysts (medium-pressure mercury UV lamp, UV light range (250–400 nm)).

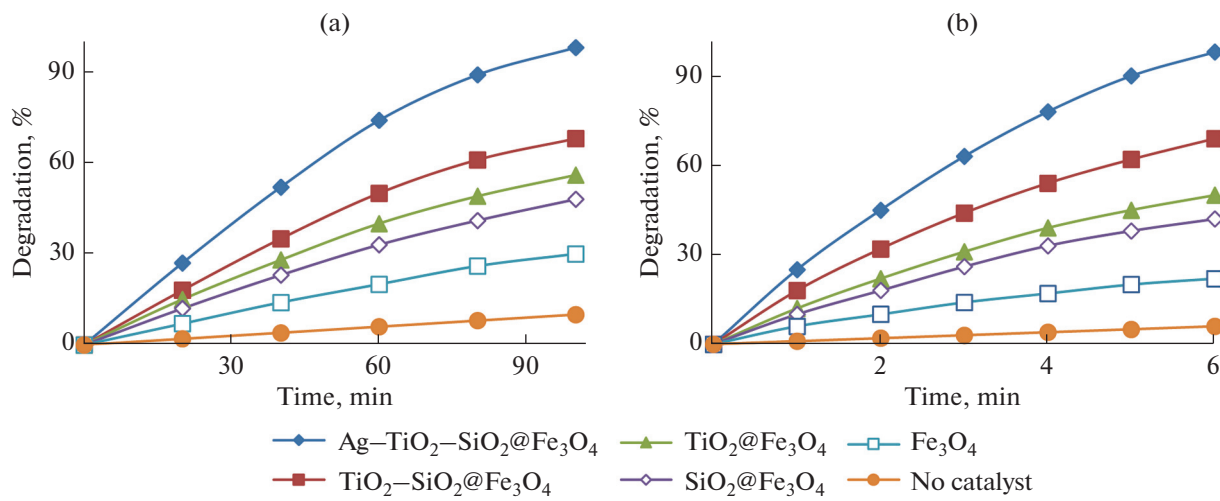
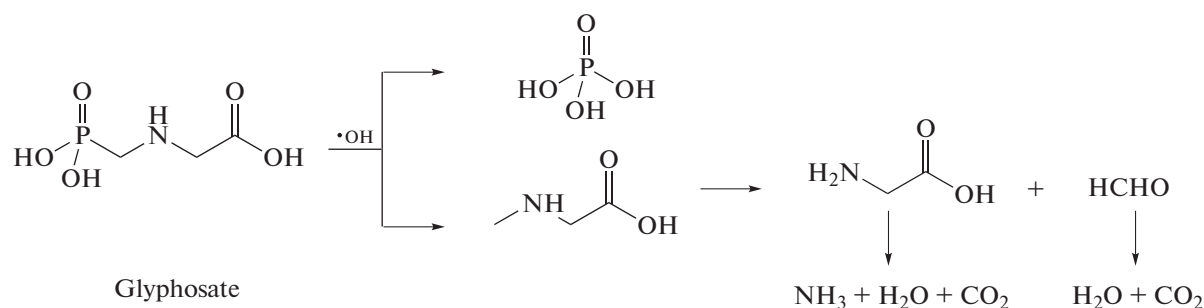
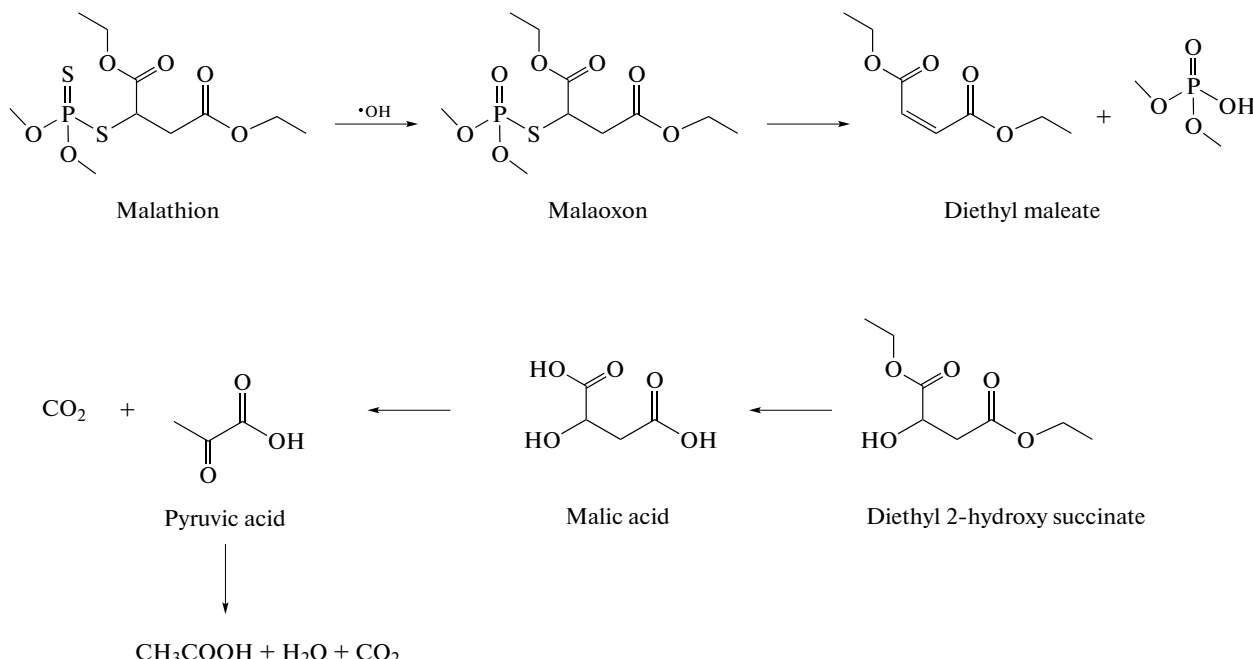


Fig. 5. Photodegradation study of (a) Glyphosate and (b) Malathion.

Glyphosate decomposition products. The possible photodecomposition pathway of Glyphosate on the Ag-TiO₂-SiO₂@Fe₃O₄ catalyst is shown below in Fig. 6. Oxidative degradation due to hydroxyl radical may lead to complete mineralization of Glyphosate through glycine formation and its further decomposition to CO₂ and H₂O.

Malathion decomposition products. The possible photodecomposition pathway of Malathion on the Ag-TiO₂-SiO₂@Fe₃O₄ catalyst by oxidative degradation due to hydroxyl radical is shown below in Fig. 7. Malathion may undergo stepwise degradation through the formation of malaoxon, diethyl maleate, diethyl-2-hydroxy succinate, malic acid, pyruvic acid, and be completely mineralized further to CO₂ and H₂O.

**Fig. 6.** Photodegradation pathway of Glyphosate.**Fig. 7.** Photodegradation pathway of Malathion.

The Study of the Effect of Various Parameters

Chemical oxidant. We performed the degradation reactions in the presence of the chemical oxidant H₂O₂. The rate of degradation was found to increase drastically in the presence of H₂O₂; hence, the method was an advanced oxidation technique.

pH. The model reaction was performed at various pH (1–14) using the Ag-TiO₂-SiO₂@Fe₃O₄ catalyst with H₂O₂ as the oxidant. The degradation of pesticides achieved better results in the pH range from 6 to 8. We observed that at pH 6.5, the rate of photocatalytic degradation reaction was highest. The rate of degradation decreases drastically at pH < 5 and pH > 9. In the case of photocatalytic reactions on semiconducting photocatalysts, pH plays a crucial role as the reaction mechanism involves hydroxyl radical attack, direct oxidation by the positive hole and direct reduction by the electron in the conducting band.

At about pH 6, the surface of the semiconducting material becomes positively charged and strongly adsorbs the pesticides, resulting in a higher degradation rate. Formation of hydroxyl radicals due to the decomposition of hydrogen peroxide favours at about pH 6.5 on semiconducting metal oxides. The rate of degradation decreases drastically at pH < 5 and pH > 9 may be because below pH 5 and above pH 9, hydroxyl radical formation is suppressed which is necessary to carry out oxidative degradation of pesticides [23].

Temperature. All the reactions were performed at about 40–50°C: no external temperature was supplied. It was the auto-generated temperature produced under UV irradiation.

Reusability and recyclability of the catalyst. Since the catalyst was magnetically separable, it was separated using a magnet after each degradation reaction and reused for next cycle directly without further washing treatment. The catalyst $\text{Ag}-\text{TiO}_2-\text{SiO}_2@\text{Fe}_3\text{O}_4$ was recycled for ten subsequent cycles and found to be recyclable without appreciable loss in its catalytic efficiency.

The COD values of samples prepared initially ranged from 450–500 mg/L in terms of dissolved oxygen content in 50 mL of diluted solution. After the open reflux reaction with potassium dichromate solution for COD measurements, the COD value was found to decrease to the range of 5–10 mg/L for different samples following the photocatalytic degradation of pesticides with $\text{Ag}-\text{TiO}_2-\text{SiO}_2@\text{Fe}_3\text{O}_4$. The complete decomposition of the starting material was also confirmed using HPLC analysis.

CONCLUSIONS

In conclusion, we have developed an efficient method for the photodegradation of organophosphorus pesticides using $\text{Ag}-\text{TiO}_2-\text{SiO}_2@\text{Fe}_3\text{O}_4$. The addition of Ag enhances the photocatalytic efficiency of $\text{TiO}_2-\text{SiO}_2@\text{Fe}_3\text{O}_4$, making the doped catalyst superior for the degradation of Glyphosate and Malathion in water with H_2O_2 oxidant under UV irradiation. This core-shell nanocatalyst is magnetically separable and recyclable for ten subsequent cycles, showing no appreciable loss in catalytic efficiency. Additionally, no leaching of silver and iron metal ions was observed during the reaction.

FUNDING

This study was supported by the University of Mumbai through a minor research grant funding scheme (project no. 287).

CONFLICT OF INTEREST

The authors of this work declare that they have no conflicts of interest.

REFERENCES

1. Akhtar, M.W., Sengupta, D., and Chowdhury, A., Impact of pesticides use in agriculture: Their benefits and hazards, *Interdiscip. Toxicol.*, 2009, vol. 2, pp. 1–12.
<https://doi.org/10.2478/v10102-009-0001-7>
2. Levine, M.J., *Pesticides: A Toxic Time Bomb in Our Midst*, London: Bloomsbury, 2007.
3. Muñoz-Quezada, M.T., Lucero, B.A., Iglesias, V.P., Muñoz, M.P., Cornejo, C.A., Achu, E., Baumert, B., Hanchey, A., Concha, C., Brito, A.M., and Villalobos, M., Chronic exposure to organophosphate (OP) pesticides and neuropsychological functioning in farm workers: A review, *Int. J. Occup. Environ. Health*, 2016, vol. 22, pp. 68–79.
<https://doi.org/10.1080/10773525.2015.1123848>
4. Sapkal, B., Labhane P., and Satam, J., In water–ultrasound-promoted synthesis of tetraketones and 2-substituted-1-H-benzimidazol catalyzed by BiOCl nanoparticles, *Res. Chem. Intermed.*, 2017, vol. 43, pp. 4967–4979.
<https://doi.org/10.1007/s11164-017-2924-5>
5. Satam, J.R., Gawande, M.B., Deshpande, S.S., and Jayaram, R.V., $\text{SO}_4^{2-}/\text{SnO}_2$: Efficient, chemoselective and reusable catalyst for the acylation of alcohols, phenols and amines, *Synth. Commun.*, 2007, vol. 37, pp. 3011–3020.
<https://doi.org/10.1080/00397910701354723>
6. Satam, J.R., and Jayaram, R.V., Selective procedure for the conversion of alcohols into alkyl iodides with $\text{SO}_4^{2-}/\text{ZrO}_2$ and NaI at room temperature, *Catal. Commun.*, 2008, vol. 6, pp. 1033–1039.
<https://doi.org/10.1016/j.catcom.2007.10.004>
7. Rabindranathan, S., Devipriya, S., and Yesodharan, S., Photocatalytic degradation of phosphamidon on semiconductor oxides, *J. Hazard. Mater.*, 2003, vol. 102, pp. 217–229.
[https://doi.org/10.1016/S0304-3894\(03\)00167-5](https://doi.org/10.1016/S0304-3894(03)00167-5)
8. Mahalakshmi, M., Palanichamy, M., Banumathi, A., and Murugesan, V., Photocatalytic degradation of carbofuran using semiconductor oxides, *J. Hazard. Mater.*, 2007, vol. 143, pp. 240–245.
<https://doi.org/10.1016/j.jhazmat.2006.09.008>
9. Gaya, U.I. and Abdullah, A.H., Heterogeneous photocatalytic degradation of organic contaminants over titanium dioxide: A review of fundamentals, progress and problems, *J. Photochem. Photobiol. C*, 2008, vol. 9, pp. 1–12.
<https://doi.org/10.1016/j.jphotochemrev.2007.12.003>

10. Cherepivska, M.K., and Prihod'ko, R.V., Sol-gel synthesized semiconductor oxides in photocatalytic degradation of phenol, *ISRN Phys. Chem.*, 2013, vol. 2014, p. 724095.
<https://doi.org/10.1155/2014/724095>
11. Anpo, M., Utilization of TiO₂ photocatalysts in green chemistry, *Pure Appl. Chem.*, 2000, vol. 72, pp. 1265–1270.
<https://doi.org/10.1351/pac200072071265>
12. Chen, D., and Gao, L., A facile route for high-throughput formation of single-crystal α-Fe₂O₃ nanodisks in aqueous solutions of Tween 80 and triblock copolymer, *Chem. Phys. Lett.*, 2004, vol. 395, pp. 316–320.
<https://doi.org/10.1016/j.cplett.2004.07.102>
13. Vaya, D., and Surolia, P.K., Semiconductor based photocatalytic degradation of pesticides: An overview, *Environ. Technol. Innovation*, 2020, vol. 20, p. 101128.
<https://doi.org/10.1016/j.eti.2020.101128>
14. Adams, C.D., and Kuzhikanni, J.J., Effect of UV/H₂O₂ preoxidation on the aerobic biodegradability of quaternary amine surfactants, *Water Res.*, 2000, vol. 34, pp. 668–672.
[https://doi.org/10.1016/S0043-1354\(99\)00186-4](https://doi.org/10.1016/S0043-1354(99)00186-4)
15. Oturan, M.A. and Aaron, J.J., Advanced oxidation processes in water/wastewater treatment: Principles and applications. A review, *Crit. Rev. Environ. Sci. Technol.*, 2014, vol. 44, pp. 2577–2641.
<https://doi.org/10.1080/10643389.2013.829765>
16. Rodríguez-Chueca, J., Carballo, J., and García-Muñoz, P., Intensification of photo-assisted advanced oxidation processes for water treatment: A critical review, *Catalysts*, 2023, vol. 13, p. 401.
<https://doi.org/10.3390/catal13020401>
17. Alfano, O.M., Bahnemann, D., Cassano, A.E., Dillert, R., and Goslich, R., Photocatalysis in water environments using artificial and solar light, *Catal. Today*, 2000, vol. 58, pp. 199–230.
[https://doi.org/10.1016/S0920-5861\(00\)00252-2](https://doi.org/10.1016/S0920-5861(00)00252-2)
18. Amine, A., Boulkamh, A., and Richard, C., Photo-transformation of metobromuron in the presence of TiO₂. *Appl. Catal. B: Environ.*, 2005, vol. 59, pp. 147–154.
<https://doi.org/10.1016/j.apcatb.2005.01.010>
19. Varanasi, P., Fullana, A., and Sidhu, S., Remediation of PCB contaminated soils using iron nano-particles, *Chemosphere*, 2007, vol. 66, pp. 1031–1038.
<https://doi.org/10.1016/j.chemosphere.2006.07.036>
20. Siddique, M., Farooq, R., and Price, G.J., Synergistic effects of combining ultrasound with the Fenton process in the degradation of Reactive Blue-19, *Ultrason. Sonochem.*, 2014, vol. 21, pp. 1206–1212.
<https://doi.org/10.1016/j.ultsonch.2013.12.016>
21. Długosz, O., Szostak, K., Krupiński, M., and Banach, M., Synthesis of Fe₃O₄/ZnO nanoparticles and their application for the photodegradation of anionic and cationic dyes, *Int. J. Environ. Sci. Technol.*, 2021, vol. 18, pp. 561–574.
<https://doi.org/10.1007/s13762-020-02852-4>
22. Sun, W., Wang, S., Yu Z., and Cao, X., Characteristics and application of iron-based materials in heterogeneous Fenton oxidation for wastewater treatment: A review, *Environ. Sci.: Water Res. Technol.*, 2023, vol. 9, pp. 1266–1289.
<https://doi.org/10.1039/D2EW00810F>
23. Nakabayashi, Y., and Nosaka, Y., The pH dependence of OH radical formation in photo-electrochemical water oxidation with rutile TiO₂ single crystals, *Phys. Chem. Chem. Phys.*, 2015, vol. 17, pp. 30570–30576.
<https://doi.org/10.1039/c5cp04531b>

Publisher's Note. Allerton Press remains neutral with regard to jurisdictional claims in published maps and institutional affiliations.